Wireless Power Transfer in Distributed Antenna Systems

Abdelhamid Salem, *Student Member, IEEE*, Leila Musavian, *Member, IEEE*, and Khairi Ashour Hamdi, *Senior Member, IEEE*

***Abstract*— This paper studies the performance of wireless power transfer in distributed antenna systems (DAS). In particular, the distributed remote radio heads (RRHs), which are conventionally distributed in the network to enhance the performance, are also used to increase the energy harvesting (EH) at the energy-constrained users. Based on this idea, the network area is divided into two zones, namely: 1) EH zone and 2) interference zone. The users in the EH zones are guaranteed to harvest sufficient energy from the closed RRH, while the users in the interference zones harvest energy from the surrounding RRHs. A harvest-then-transmit protocol is adopted, where in the power transfer phase the multiple antennas RRHs broadcast energy signals to the users. In the information transmission phase, the users utilize the harvested energy to transmit their signals to the RRHs. In addition, zero-forcing is applied at the RRHs receivers, to mitigate the interference. The system spectral efficiency is evaluated in two different scenarios based on the channel state information (CSI) namely: 1) CSI is unknown at the RRHs 2) CSI is perfectly known at the RRHs. In contrast to conventional EH-muliple-input multiple-output (MIMO) systems, performance analysis of EH DAS-MIMO is a challenging problem, because the channels are characterized by non-identical path-loss and EH effects which make the classical analytical methods non-tractable. In light of this, new analytical expressions of the ergodic spectral efficiency are derived and then Monte Carlo simulations are provided to verify the accuracy of our analysis. The effects of main system parameters on the EH-DAS performance are investigated. The results show that there is an optimal value of the EH time for each users locations that maximizes the system performance. In addition, size of the EH-zone area depends on the required harvested power at the users which is dependent essentially on the target spectral efficiency.**

***Index Terms*— DAS, wireless power transfer, zero forcing, spectral efficiency, CSI.**

I. Introduction

RADIO frequency (RF) energy harvesting (EH) in wireless communication networks has attracted significant research attention in recent years [1]–[4]. This concept depends on the fact that RF signals are able to transfer energy to the nodes in wireless communication systems. Consequently, considerable amount of works have been achieved to study the efficiency of wireless-powered communication networks (WPCNs), in which the energy signals are exploited to charge the EH-nodes in the network. For instance, a tradeoff between the information and energy can be sent over a noisy and frequency selective channels with additive white Gaussian noise (AWGN) were considered in [1] and [2], respectively. Multiple-antenna techniques have been also used to further increase the performance of WPCNs. The efficiency of multi-antenna WPCN with energy beam-forming was investigated in [5]. A system model consisting of multiple EH-nodes communicating with an access point (AP), where in the first phase, down-link (DL), the AP transmits energy signals to the EH-nodes, and then in the second phase, up-link (UL), the EH-nodes transmit their data to the AP using the harvested energy was considered in [6] and [7]. This protocol is called harvest-then-transmit protocol. Theses works were extended in [8] and [9] to include a multi-antenna AP. RF-EH power splitting technique for a multiple input single output (MISO) systems with quality of service constraint and EH constraint was considered in [10], where the minimum required power was formulated for both variable/constant beamforming weights at the transmitters. In addition, the problem of joint transceiver design for full duplex cloud radio access systems with simultaneous wireless information and power transfer was studied in [11]. For some new research trends in wireless powered communication networks, we refer the reader to [12].

Moreover, distributed antenna system (DAS) has been proposed to improve the spectral efficiency, power efficiency and to extend the service coverage area of the communication networks [13]–[16]. In DAS, the functionalities of the base station or the AP are divided between a central processor unit (CPU) and a group of low-cost remote radio heads (RRHs). Practically, the CPU performs the base-band signal processing and the RRHs are responsible for all RF operations [13]. The RRHs are geographically distributed in a cell area to reduce the access distances and the total transmission power. It was shown in literature that, DAS with full cooperation between the transmitters has a better performance than the conventional collocated antenna systems (CAS) [14], [15]. In [17], the performance of the distributed multi-input multi-output (D-MIMO) system and conventional collocated MIMO (C-MIMO) system were investigated and compared.

Manuscript received October 27, 2017; revised April 28, 2018 and July 21, 2018; accepted August 7, 2018. Date of publication August 14, 2018; date of current version January 15, 2019. This work is supported By the UK EPSRC under grant EP/N032268/1. The associate editor coordinating the review of this paper and approving it for publication was H. R. Bahrami. *(Corresponding author: Abdelhamid Salem.)*

A. Salem is with the Department of Electronic and Electrical Engineering, University College London, London WC1E 7JE, U.K. (e-mail: a.salem@ucl.ac.uk).

L. Musavian is with the School of Computer Science and Electronic Engineering, University of Essex, Colchester CO4 3SQ, U.K. (e-mail: leila.musavian@essex.ac.uk).

K. A. Hamdi is with the School of Electrical and Electronic Engineering, The University of Manchester, Manchester M13 9PL, U.K. (e-mail: k.hamdi@manchester.ac.uk).

Color versions of one or more of the figures in this paper are available online at http://ieeexplore.ieee.org.

Digital Object Identifier 10.1109/TCOMM.2018.2865481

New expressions for the ergodic spectral efficiency of C-MIMO system and D-MIMO system were derived and compared in [18]. New algorithms to determine the antenna position for down-link DASs in single and two cell environments were proposed in [19]. In addition, a comparative study on the ergodic sum rate of cellular networks in up-link scenario was presented in [20], where the antennas of the BS are located at the center of a cell or uniformly distributed in the cell area. In [21], a transmit optimization method was proposed to maximize the energy efficiency of DAS. A beam-forming and power allocation algorithm for a down-link MISO-DAS which maximizes the energy efficiency was proposed in [22]. In [23] the ergodic capacity of down-link DAS was investigated, where each RRH equipped with multiple antennas.

A. Related Works

Wireless power transfer technique has been considered in DAS, recently, in several works. In detail, a resource allocation algorithm design for information and power transfer to mobile receivers in DAS was studied in [13], in which the RRHs and CPU are equipped with renewable energy harvesters. Only the down-link scenario was considered in [13], when the system consists of two types of receivers, information and EH receivers. Tabassum and Hossain [24] theoretically characterized the outage zones in wireless power systems and analyzed the performance of different configurations of the energy sources which can minimize the outage zones; In the considered system, the users harvest energy from symmetrically deployed power beacons in down link, and transmit their information signals to the base station (BS) in the uplink phase. A distributed antenna power beacon (DA-PB) was proposed in [25], in which DA-PB antennas are uniformly distributed in a cell area. In this work the authors assumed that the PB has no knowledge of the users' CSI, and closed form expression of the average harvested power per user was derived. In [26], energy efficiency in downlink EH-DAS was studied, where each RRH is equipped with only a single antenna, and power splitting technique was implemented at the EH-devices to achieve the EH and information processing. In this work [26], closed form expression for the energy efficiency in the case of a single device was derived, and an efficient suboptimal algorithm to find the optimal energy efficiency for the case of multiple devices was proposed. Simultaneous wireless information and energy transfer in only down-link DAS was considered in [27], in which the cooperation of EH and two-way energy flows to make the distributed remote antenna units trade their harvested energy through a smart grid network were adopted to save the energy cost. Under some EH constraints, per remote antenna power constraints, and different smart grid configurations, a power management policy that finds how to use the harvested energy at the remote antenna units and how to trade the energy with the smart grid to achieve maximum wireless information transfer with a minimum wireless energy transfer constraint was obtained in [27]. Practical and efficient channel training techniques to perform optimal energy beamforming in a distributed wireless energy transfer systems were studied in [28]. The concept of wireless power and information transfer in massive DASs to enhance the mobile networks was introduced in [29]. Specifically, the massive distributed antenna system (MDAS) was implemented to improve both the wireless energy and information transfer. In this work the authors presented and discussed some research trends in MDAS involving wireless energy and information transfer. Wang *et al.* [30] considered the secrecy in downlink DAS with wireless energy and information transfer, in which the user implements power splitting receiver to harvest energy and process the information simultaneously; Closed form expression for the transmitted information signal power that maximizes the system secrecy and energy harvesting was derived in this work.

B. Contributions

Motivated by the aforementioned discussions, in this paper, we propose the use of distributed RRHs also to power the energy-constrained users wirelessly. More specifically, the RRHs are distributed in the network, where each RRH has an EH zone with a radius satisfying the threshold requirements of the EH circuit, and any user within this region can harvest a sufficient amount of energy and communicate reliably with the closest RRH. On the other hand, any user outside the EH zones, will be in interference zone where the amount of the harvesting energy depends on the received RF energy signals from all the RRHs. Harvest-then-transmit protocol is adopted in this paper. Hence, the information transmission in the proposed system achieved in two time slots:

1) Phase I: in this time slot all the RRHs broadcast independent RF energy signals, the energy of these signals is harvested by the all users to charge their batteries.
2) Phase II: in this time slot all EH-users send their information signals to the RRHs by using the harvested power.

In addition, zero-forcing (ZF) receiver is implemented at the RRHs in the second phase, in order to mitigate the interference between the users' signals and to enhance the system performance.[1] The ergodic spectral efficiency is adopted as a performance measure to characterize the network performance. Practically, accurate channel state information (CSI) at the RF energy source in EH systems, before power transmission might be difficult to achieve. This is because accurate channel estimation consumes considerable amount of the harvested energy. Therefore, the ergodic spectral efficiency is studied in two cases based on the CSI at the RRHs in the first phase, namely, 1) CSI is unknown at the RRHs; 2) CSI is perfectly known at the RRHs.[2]

It is known that, the performance analysis of EH DAS-MIMO system with ZF receiver is difficult and challenging, since the overall signal to interference and noise ratio includes sum of non-identical matrices instead of only one as in conventional-MIMO systems. Also, transmitting power of the users is random depending on the small scale-fading, which makes the analysis of this model hard and challenging.

Therefore, the major contributions of this work are summarized as follows:

[1]ZF scheme is selected, because it is simple and ease of implementation.
[2]The impact of imperfect CSI, will be investigated in future work.

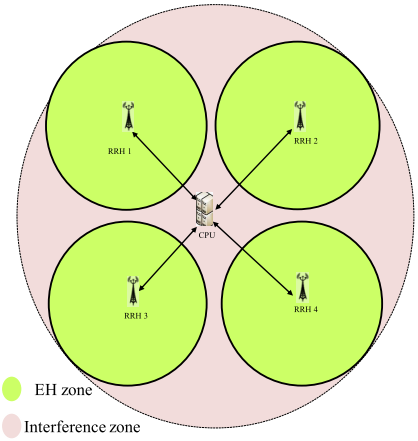

Fig. 1. EH-distributed antenna system with EH and interference zones.

1) New analytical expression for the up-link spectral efficiency of EH MIMO-DAS system with ZF receiver is derived and presented over independent Rayleigh fading channels, when the CSI is unknown in the first phase.
2) New analytical expression for the upper bound of the up-link spectral efficiency of the EH MIMO-DAS system with ZF receiver is derived and presented over independent Rayleigh fading channels, when the CSI is fully-known, and maximum-ratio transmission (MRT) technique is used to maximize the harvested power at the EH-users during the first phase.
3) Monte-Carlo simulations are also provided to confirm the accuracy of our analysis, and then we investigate the effects of several main parameters on the system performance.

The remaining sections of this paper are organized as follows. In Section II we present the system model. In Sections III and IV we derive analytical expressions for the ergodic spectral efficiency when the CSI in the first phase is un-known and fully-known, respectively. Next, in Section V, numerical results and system performance evaluation are shown and discussed. Finally, the main conclusions of this work are stated in section VI.

II. System Model

We consider a DAS system consisting of L RRHs each of which is equipped with N_r antennas. All RRHs are assumed to have a separate feeder to the CPU. As mentioned in the introduction, the RRHs are distributed in the network to provide coverage and wireless energy to the users in the network. Each RRH has an EH zone in circular shape with a radius, r, satisfying the threshold requirements of the EH circuit. All users in the EH zones can harvest sufficient amount of energy and communicate reliably with the closed RRH. However, users outside the EH zones, considered to be in interference zone, as shown in Fig. 1. Number of the single antenna users in the network is N_s, where $N_r > N_s$. All the channels in this paper are considered to be independent identically distributed (i.i.d) follow Rayleigh fading magnitude, this assumption is widely adopted

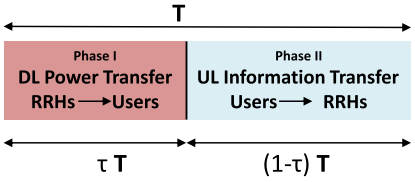

Fig. 2. Harvest-then-transmit protocol.

in MIMO systems.[3] The total $N_s \times LN_r$ channel matrix between the RRHs and the users in the first time slot, power transfer phase, is denoted by $\mathbf{G}$, which is consisting of L independent sub-channel matrices for all RRHs, $\mathbf{G} = [\mathbf{G}_1\mathbf{G}_2.....\mathbf{G}_L]^t$, where $\mathbf{G}_l, l = 1, 2, ..., L$, is the $N_s \times N_r$ channel matrix between the l^{th} RRH and the users in its coverage and t denotes the transpose operation. The all channel matrices composed of small and large scale fading, $\mathbf{G}_l = \mathbf{D}_l^{1/2}\mathbf{R}_l$ where $\mathbf{R}_l$ contains i.i.d, complex-Gaussian distribution with zero mean and unity variance entries, i.e., $\mathcal{CN}(0, 1)$, which represents small scale fading coefficients and $\mathbf{D}_l$ is a diagonal matrix with a (k, k) element given by $[\mathbf{D}_l]_{kk} = \varpi_{lk}$ which represents the path-loss attenuation $\varpi_{lk} = d_{lk}^{-m}$, with d_{lk} denoting the distance between the l^{th} RRH and the k^{th} user and m indicating the path loss exponent. The $LN_r \times N_s$ channel matrix in the second phase is represented by $\mathbf{H}$, which includes L independent sub-channel matrices. The channel matrix between the l^{th} RRH and the users is, $\mathbf{H}_l = \mathbf{F}_l\mathbf{D}_l^{1/2}$ where $\mathbf{F}_l$ contains i.i.d $\mathcal{CN}(0, 1)$ entries representing small scale fading coefficients. In addition, it is assumed that the total available system power, P_T, is equally divided between all RRHs, therefore, this assumption provides a lower-bound on the performance of practical systems. We also assume that, each user is equipped with a rechargeable battery, and the harvest-then-transmit protocol, studied in [7] and illustrated in Fig. 2, is adopted in this paper. In Fig. 2, T is the total transmission time. In this protocol, in the first time slot, τT, $0 < \tau < 1$, all RRHs transmit independent RF energy signals to all users in the network and during the second time slot, $(1-\tau)T$, all users send their independent information signals to the RRHs using the harvested power in the first time slot.

Next, the ergodic spectral efficiency is studied for two different scenarios based on the availability of the CSI at the transmitter in power transfer phase, i.e., unknown CSI and perfectly known CSI at the RRHs. In practice, accurate knowledge of the CSI at the energy transmitter in energy harvesting systems, before power transmission, is difficult to achieve.This is because accurate channel estimation consumes considerable amount of the harvested energy. Therefore, the difference between the two cases is based on the ability of the users to help the transmitter to know the channels before energy transmission [32]. For the unknown CSI case, the transmitter can know the full CSI only in the second time slot after charging the users, as studied in [33]. On the other hand, if the users can help the transmitter to estimate their channels before

[3]The uplink and downlink channels are considered to be uncorrelated. Such scenario occurs in frequency-division duplex (FDD) systems, when the frequency separation is larger than the channel coherence bandwidth [31].

power transmission. In this case, the transmitter can know fully the users' CSI, and then the transmitter can know the CSI in the second time slot after charging the users, as studied in [33]. Recently, many works have investigated the availability of the CSI at the energy transmitter in power transfer phase, for instance [32]–[35].

III. CSI Is Un-Known in the Power Transfer Phase

In this section, it is assumed that, the users' CSI is unknown at the CPU in the power transfer phase.The un-known CSI case is investigated in this work, in order to explain the impact of the channel knowledge in power transfer phase on the system performance and to gain an understanding of the idea of dividing the network area into two zones (EH and interference zones) in such scenarios. The received signal at the k^{th} user in the EH phase can hence be expressed as[4]

$$y_k = \sqrt{\frac{P}{N_r}} \sum_{i=1}^{L} \mathbf{g}_{ik}^t \mathbf{s}_{ri} + n_k, \tag{1}$$

where P is the RRH transmission power, $\mathbf{g}_{ik}$ is the $N_r \times 1$ channel coefficients vector between the i^{th} RRH and the k^{th} user, $\mathbf{s}_{ri}$ is the transmitted RF energy-signals vector; the energy-signals are i.i.d with zero mean and unity variance, and n_k is the AWGN at the k^{th} user with zero mean and σ_k^2 variance, $n_k \sim \mathcal{CN}\left(0, \sigma_k^2\right)$. Therefore, by ignoring the small amount of the noise energy, the harvested energy by the k^{th} user can be expressed as [9] and [36]

$$E_k = \frac{\eta \tau T P}{N_r} \sum_{i=1}^{L} \left\| \mathbf{g}_{ik}^t \right\|^2, \tag{2}$$

where η denotes the efficiency of the EH-receiver $0 < \eta \leq 1$ and $\|.\|$ is the Euclidean norm. Amount of the harvested power at the user k can be calculated as[5] [8] and [9]

$$P_k = \frac{E_k}{(1-\tau)\, T} = \frac{\eta \tau P}{(1-\tau)\, N_r} \sum_{i=1}^{L} \left\| \mathbf{g}_{ik}^t \right\|^2. \tag{3}$$

The transmitted signal of the k^{th} user in the information transmission phase is

$$x_k = \sqrt{P_k} s_k, \tag{4}$$

where s_k is the transmitted data signal of the k^{th} user; the users' signals in the information transmission phase are i.i.d. with zero mean and unity variance. In the up-link, users send their signals to the RRHs, the received signal at the CPU is given by

$$\mathbf{y}_d = \mathbf{H}\mathbf{x} + \mathbf{n}_d, \tag{5}$$

where $\mathbf{x} = \left[\sqrt{P_1} s_1, \sqrt{P_2} s_2, ..., \sqrt{P_{N_s}} s_{N_s}\right]^t$ and $\mathbf{n}_d$ is the AWGN vector at the CPU with $\mathbf{n}_d \sim \mathcal{CN}\left(0, \sigma_d^2 \mathbf{I}_{LN_r}\right)$, while $\mathbf{I}_{LN_r}$ is the identity matrix. By applying the ZF decoder at the CPU, the interference is completely removed and the received signals can be separated by using the weight matrix $\mathbf{W} = \left(\mathbf{H}^H \mathbf{H}\right)^{-1} \mathbf{H}^H$, where $(.)^H$ is the conjugate transpose operation. Consequently, (5) can now be written as

$$\mathbf{y}_d = \mathbf{x} + \mathbf{W}\mathbf{n}_d, \tag{6}$$

Then, the k^{th} received signal is expressed as

$$y_{dk} = \sqrt{P_k} s_k + [\mathbf{W}]_k \, \mathbf{n}_d, \tag{7}$$

where $[\mathbf{A}]_k$ is the vector k in matrix $\mathbf{A}$. Therefore, the received signal to noise ratio (SNR) at the k^{th} ZF output is equal to

$$\gamma_k = \frac{P_k}{\sigma_d^2 \left[\left(\mathbf{H}^H \mathbf{H}\right)^{-1}\right]_{k,k}}, \tag{8}$$

where $[\mathbf{A}]_{k,k}$ is the element (k,k) in matrix $\mathbf{A}$. Substituting (3) into (8), the SNR can be written as

$$\gamma_k = \frac{\frac{\eta \tau P}{(1-\tau) N_r} \sum\limits_{i=1}^{L} \left\| \mathbf{g}_{ik}^t \right\|^2}{\sigma_d^2 \left[\left(\mathbf{H}^H \mathbf{H}\right)^{-1}\right]_{k,k}}. \tag{9}$$

Now, the spectral efficiency of EH-DAS can be given by

$$C = (1-\tau) \sum_{k=1}^{N_s} \log_2 \left(1 + \gamma_k\right), \tag{10}$$

where $\log_2(.)$ represents logarithm of base-2. Substituting (9) into (10) yields

$$C = (1-\tau) \sum_{k=1}^{N_s} \log_2 \left(1 + \frac{a \sum\limits_{i=1}^{L} \left\| \mathbf{g}_{ik}^t \right\|^2}{\left[\left(\mathbf{H}^H \mathbf{H}\right)^{-1}\right]_{k,k}} \right), \tag{11}$$

where $a = \frac{\eta \tau P}{\sigma_d^2 (1-\tau) N_r}$. Now the ergodic spectral efficiency can be written as

$$\bar{C} = (1-\tau) \sum_{k=1}^{N_s} \mathbb{E}\left[\log_2 \left(1 + \frac{a \sum\limits_{i=1}^{L} \left\| \mathbf{g}_{ik}^t \right\|^2}{\left[\left(\mathbf{H}^H \mathbf{H}\right)^{-1}\right]_{k,k}} \right) \right], \tag{12}$$

$$= (1-\tau) \sum_{k=1}^{N_s} \mathbb{E}\left[\log_2 \left(1 + \frac{X}{Y} \right) \right], \tag{13}$$

where $\mathbb{E}[.]$ is the expectation operation, $X = a \sum\limits_{i=1}^{L} \left\| \mathbf{g}_{ik}^t \right\|^2$ and $Y = \left[\left(\mathbf{H}^H \mathbf{H}\right)^{-1}\right]_{k,k}$.

The ergodic spectral efficiency can be calculated using the following Lemma.

Lemma 1: It is found in [36] that for any arbitrary non-negative random variables $x, y > 0$,

$$\mathbb{E}\left[\log_2 \left(1 + \frac{x}{y} \right) \right] = \int_0^{\infty} \frac{1}{z \ln(2)} \left(\mathcal{M}_y(z) - \mathcal{M}_{x,y}(z) \right) dz, \tag{14}$$

[4] At the beginning, we generalize the analysis by assuming that the users in the EH zones can receive energy from the all RRHs. The case where each user in EH zone harvests energy and transmits its data from/to the closed RRH only, can be easily obtained by using only one RRH in the derived expressions, this case is considered in Section V.

[5] As mentioned previously, the harvested energy at each user in EH zone from its RRH, i.e, the closed RRH to the user, is assumed to be sufficient for the up-link transmission

where $\ln(.)$ represents logarithm of base e, $\mathcal{M}_y(z)$ and $\mathcal{M}_{x,y}(z)$ are the moment generating functions (MGFs) of the random variables y and $x+y$, respectively, which are defined as $\mathcal{M}_y(z) = \mathbb{E}[e^{-zy}]$ and $\mathcal{M}_{x,y}(z) = \mathbb{E}\left[e^{-z(x+y)}\right]$.

Proof: The proof of this Lemma is provided in [36]. ■

Invoking the definition in (14), (13) can be written as

$$\bar{C} = \frac{(1-\tau)}{\ln(2)} \sum_{k=1}^{N_s} \int_0^{\infty} \frac{1}{z} \left(\mathcal{M}_Y(z) - \mathcal{M}_Y(z)\, \mathcal{M}_X(z) \right) dz, \quad (15)$$

where $\mathcal{M}_X(z)$ and $\mathcal{M}_Y(z)$ are the MGFs of X and Y, receptively. Since X is the summation of independent Gamma random variables, its MGF can be found as

$$\mathcal{M}_X(z) = \prod_{i=1}^{L} (1 + a\varpi_{ik} z)^{-N_r}. \quad (16)$$

From [9] and [38] $\mathcal{M}_Y(z)$ can be expressed as

$$\mathcal{M}_Y(z) = \frac{2(\theta z)^{\frac{\Theta N_r - N_s + 1}{2}}\ \mathrm{J}\left(\Theta N_r - N_s + 1, 2\sqrt{\theta z}\right)}{\Gamma(\Theta N_r - N_s + 1)}, \quad (17)$$

where $\Theta = \frac{\left(\sum_{i=1}^{L} \varpi_{ik}\right)^2}{\sum_{i=1}^{L} \varpi_{ik}^2}$, $\theta = \frac{\sum_{i=1}^{L} \varpi_{ik}}{\sum_{i=1}^{L} \varpi_{ik}^2}$, and J (.) is the modified Bessel function of the second kind [38]. Substituting (16) and (17) into (15), the ergodic spectral efficiency of EH-DAS system with ZF receiver can be obtained as in (18), as shown at the bottom of this page.

(18) is an explicit expression for the ergodic spectral efficiency, since for mathematical tractability Gaussian Quadrature rule can be applied. Therefore, the ergodic spectral efficiency of EH-DAS system with ZF receiver can be also written as (19), as shown at the bottom of this page, where z_j and H_j are the j^{th} abscissa and weight of the n^{th} order Laguerre polynomial [38, eq. (25.4.45)]. From this expression, the effect of different system parameters on the spectral efficiency can be obviously observed. Therefore, the ergodic spectral efficiency with respect to each user location can be derived by averaging the spectral efficiency in (19) over all user positions.

Remark 1: Since $\|\mathbf{g}_{ik}\|^2$ has Gamma distribution. The average harvested power can be written as

$$\bar{P}_k = \frac{\eta\tau P_{nr} N_r \sum_{i=1}^{L} \varpi_{ik}}{(1-\tau)}, \quad (20)$$

where P_{nr} is the transmission power per antenna. (20) indicates that increasing N_r leads to increase in the amount of the harvested power. In addition, in case when the users in the EH zones harvest power only from its closed RRH, i.e, $L = 1$, the average harvested power simplifies to

$$\bar{P}_k = \frac{\eta\tau P_{nr} N_r \varpi_{lk}}{(1-\tau)}. \quad (21)$$

Hence, the harvested power at the k^{th} user decreases with increasing the distance between the user and the closest RRH, due to the path-loos, $\varpi_{lk} = d_{lk}^{-m}$. Therefore, the radius of any EH zone, r, can be defined using (21) and the required harvested power (P_{rq}) as [39],

$$r = \sqrt[m]{\frac{\eta\tau P_{nr} N_r}{P_{rq}(1-\tau)}}. \quad (22)$$

Thus radius of the EH zones can be obtained based on the target spectral efficiency and the system parameters such as number of the RRHs antennas and the transmission power in the power transfer phase. As a result, for a given number of RRH antennas N_r, transmission power P_{nr}, path loss exponent m and the EH efficiency η, the radius r depends on the required harvested power which is dependent mainly on the target spectral efficiency. When the target spectral efficiency is high, the required harvested power P_{rq} at a user will be high and the radius of EH zone will be small, and Vice-versa. Therefore we can say that, r denotes the boundary beyond which all EH zone users cannot provide the target spectral efficiency, and their performance depend on the received signals from other the surrounded RRHs.

IV. Full Known CSI

In this section, it is assumed the users' CSI is fully-known at the CPU in the power transfer slot. In order to maximize the harvested power, in this scenario, MRT technique is proposed. Several beam-forming and algorithms techniques have been proposed for MIMO systems to provide optimal harvested power, such as in [8] and [10]. Although, the developed techniques provided optimal solutions, its high computational complexity makes them unsuitable for real time applications. In contrast, MRT scheme has low complexity and it is suitable for the practical systems. Consequently, the received signal in the power transfer phase at the k^{th} user is

$$y_k = \sqrt{P} \sum_{l=1}^{L} \left(\mathbf{g}_{lk}^t \mathbf{w}_{lk} s_{rl,k} + \sum_{i=1, i\neq k}^{N_s} \mathbf{g}_{lk}^t \mathbf{w}_{li} s_{rl,i} \right) + n_k, \quad (23)$$

$$\bar{C} = \frac{(1-\tau)}{\ln(2)} \sum_{k=1}^{N_s} \int_0^{\infty} \frac{1}{z} \left(1 - \prod_{i=1}^{L} (1 + a\varpi_{ik} z)^{-N_r} \right) \frac{2(\theta z)^{\frac{\Theta N_r - N_s + 1}{2}}\ \mathrm{J}\left(\Theta N_r - N_s + 1, 2\sqrt{\theta z}\right)}{\Gamma(\Theta N_r - N_s + 1)} dz. \quad (18)$$

$$\bar{C} = \frac{(1-\tau)}{\ln(2)} \sum_{k=1}^{N_s} \sum_{j=1}^{n} \mathrm{H}_j \frac{e^{z_j}}{z_j} \left(1 - \prod_{i=1}^{L} (1 + a\varpi_{ik} z_j)^{-N_r} \right) \frac{2(\theta z_j)^{\frac{\Theta N_r - N_s + 1}{2}}\ \mathrm{J}\left(\Theta N_r - N_s + 1, 2\sqrt{\theta z_j}\right)}{\Gamma(\Theta N_r - N_s + 1)}. \quad (19)$$

where $\mathbf{w}_{lk}$ and $\mathbf{w}_{li}$ are the k^{th} and i^{th} vectors in the precoding matrix of the l^{th} RRH ($\mathbf{W}_l$), which is given by

$$\mathbf{W}_l = \frac{\mathbf{G}_l^H}{\sqrt{\mathbb{E}\left\{\mathrm{tr}\left(\mathbf{G}_l\mathbf{G}_l^H\right)\right\}}}, \tag{24}$$

where tr $(.)$ is the trace of a matrix. Thus, the harvested energy at user k is

$$E_k = P\eta\tau T\sum_{l=1}^{L}\left(\left|\mathbf{g}_{lk}^t\mathbf{w}_{lk}\right|^2 + \sum_{i=1,i\neq k}^{N_s}\left|\mathbf{g}_{lk}^t\mathbf{w}_{li}\right|^2\right), \tag{25}$$

where $|.|$ denotes the absolute value of a scalar. Substituting $\mathbf{w}_{lk}$, $\mathbf{w}_{li}$ in (25), and since $\left(\mathbf{G}_l\mathbf{G}_l^H\right)$ is Wishart matrix, the average of the matrix trace is $\mathbb{E}\left\{\mathrm{tr}\left(\mathbf{G}_l\mathbf{G}_l^H\right)\right\} = N_sN_r\left(\sum_{i=1}^{N_s}\varpi_{li}\right)$ [40], hence the harvested power at the k^{th} user is given by

$$P_k = \sum_{l=1}^{L}\frac{\eta\tau P\left(\left\|\mathbf{g}_{lk}^t\right\|^4 + \sum_{i=1,i\neq k}^{N_s}\left|\mathbf{g}_{lk}^t\mathbf{g}_{li}\right|^2\right)}{(1-\tau)N_sN_r\left(\sum_{i=1}^{N_s}\varpi_{li}\right)}. \tag{26}$$

which can also be written as

$$P_k = \sum_{l=1}^{L}\frac{\eta\tau P\left(\left\|\mathbf{g}_{lk}^t\right\|^4 + \left\|\mathbf{g}_{lk}\right\|^2\sum_{i=1,i\neq k}^{N_s}\frac{\left|\mathbf{g}_{lk}^t\mathbf{g}_{li}\right|^2}{\left\|\mathbf{g}_{lk}^t\right\|^2}\right)}{(1-\tau)N_sN_r\left(\sum_{i=1}^{N_s}\varpi_{li}\right)}. \tag{27}$$

Substituting (27) into (8), the SNR at the k^{th} ZF output can be expressed as in (28), as shown at the bottom of this page. Consequently, the instantaneous spectral efficiency and the ergodic spectral efficiency of EH-DAS can be written as in (29) and (30), as shown at the bottom of this page, respectively, where $a = \frac{\eta\tau P}{\sigma_d^2(1-\tau)N_sN_r}$.

Closed-form expression of the ergodic spectral efficiency in this case is hard to handle. However, since log is a concave function, we can apply Jensen's inequality, which states that $\mathbb{E}\left[\log\left(1+x\right)\right] \leq \log\left(1+\mathbb{E}\left(x\right)\right)$. Therefore, by using Jensen inequality we can obtain an upper bound of the ergodic spectral efficiency, $\left(\hat{C}\right)$, as in (31), as shown at the bottom of this page. This expression shows that, the ergodic spectral efficiency is upper-bounded by the average signal-to-noise ratio.

Based on the facts that, $\|\mathbf{g}_{lk}\|^2$and $\frac{\left|\mathbf{g}_{lk}\mathbf{g}_{li}\right|^2}{\left\|\mathbf{g}_{lk}\right\|^2}$ have Gamma and exponential distributions [41]–[43, Appendix A] and $\frac{1}{\left[\left(\mathbf{H}^H\mathbf{H}\right)^{-1}\right]_{k,k}}$ has Gamma distribution [18], the upper bound on the ergodic spectral efficiency of EH-DAS system with

$$\gamma_k = \frac{\sum_{l=1}^{L}\frac{\eta\tau P}{(1-\tau)N_sN_r\left(\sum_{i=1}^{N_s}\varpi_{li}\right)}\left(\left\|\mathbf{g}_{lk}^t\right\|^4 + \left\|\mathbf{g}_{lk}^t\right\|^2\sum_{i=1,i\neq k}^{N_s}\frac{\left|\mathbf{g}_{lk}^t\mathbf{g}_{li}\right|^2}{\left\|\mathbf{g}_{lk}^t\right\|^2}\right)}{\sigma_d^2\left[\left(\mathbf{H}^H\mathbf{H}\right)^{-1}\right]_{k,k}}. \tag{28}$$

$$C = (1-\tau)\sum_{k=1}^{N_s}\log_2\left(1 + \frac{\sum_{l=1}^{L}\frac{a}{\left(\sum_{i=1}^{N_s}\varpi_{li}\right)}\left(\left\|\mathbf{g}_{lk}^t\right\|^4 + \left\|\mathbf{g}_{lk}^t\right\|^2\sum_{i=1,i\neq k}^{N_s}\frac{\left|\mathbf{g}_{lk}^t\mathbf{g}_{li}\right|^2}{\left\|\mathbf{g}_{lk}^t\right\|^2}\right)}{\left[\left(\mathbf{H}^H\mathbf{H}\right)^{-1}\right]_{k,k}}\right). \tag{29}$$

$$\bar{C} = (1-\tau)\sum_{k=1}^{N_s}\mathbb{E}\left[\log_2\left(1 + \frac{\sum_{l=1}^{L}\frac{a}{\left(\sum_{i=1}^{N_s}\varpi_{li}\right)}\left(\left\|\mathbf{g}_{lk}^t\right\|^4 + \left\|\mathbf{g}_{lk}^t\right\|^2\sum_{i=1,i\neq k}^{N_s}\frac{\left|\mathbf{g}_{lk}^t\mathbf{g}_{li}\right|^2}{\left\|\mathbf{g}_{lk}^t\right\|^2}\right)}{\left[\left(\mathbf{H}^H\mathbf{H}\right)^{-1}\right]_{k,k}}\right)\right]. \tag{30}$$

$$\hat{C} \triangleq (1-\tau)\sum_{k=1}^{N_s}\left[\log_2\left(1 + \mathbb{E}\left\{\frac{\sum_{l=1}^{L}\frac{a}{\left(\sum_{i=1}^{N_s}\varpi_{li}\right)}\left(\left\|\mathbf{g}_{lk}^t\right\|^4 + \left\|\mathbf{g}_{lk}^t\right\|^2\sum_{i=1,i\neq k}^{N_s}\frac{\left|\mathbf{g}_{lk}^t\mathbf{g}_{li}\right|^2}{\left\|\mathbf{g}_{lk}^t\right\|^2}\right)}{\left[\left(\mathbf{H}^H\mathbf{H}\right)^{-1}\right]_{k,k}}\right\}\right)\right]. \tag{31}$$

$$\hat{C} \triangleq (1-\tau)\sum_{k=1}^{N_s}\left[\log_2\left(1 + \left(a\Theta\theta\sum_{l=1}^{L}\left(\sum_{i=1}^{N_s}\varpi_{li}\right)^{-1}\left(\varpi_{lk}^2\frac{\Gamma\left(2+N_r\right)}{\Gamma\left(N_r\right)} + \varpi_{lk}N_r\sum_{i=1,i\neq k}^{N_s}\varpi_{li}\right)\right)\right)\right]. \tag{32}$$

ZF receiver can be found as in (32), shown at the bottom of the previous page.

Remark 2: Since $\|\mathbf{g}_{lk}^t\|^2$ and $\frac{\left|\mathbf{g}_{lk}^t \mathbf{g}_{li}\right|^2}{\|\mathbf{g}_{lk}^t\|^2}$ have Gamma and exponential distributions, respectively, [41]–[43, Appendix A], the average harvested power at user k is given by

$$\bar{P}_k = \frac{\eta\tau P_{nr}}{(1-\tau)\,N_s} \sum_{l=1}^{L} \frac{\left(\varpi_{lk}^2 \frac{\Gamma(2+N_r)}{\Gamma(N_r)} + \varpi_{lk} N_r \sum\limits_{i=1, i\neq k}^{N_s} \varpi_{li}\right)}{\left(\sum\limits_{i=1}^{N_s} \varpi_{li}\right)}. \tag{33}$$

From this equation, it is clear that increasing N_r leads to increase in the amount of the harvesting power level. In the case when the users in the EH zones harvest power from only the closest RRH, i.e, $L = 1$, the average harvested power becomes

$$\bar{P}_k = \frac{\eta\tau P_{nr} \left(\varpi_{lk}^2 \frac{\Gamma(2+N_r)}{\Gamma(N_r)} + \varpi_{lk} N_r \sum\limits_{i=1, i\neq k}^{N_s} \varpi_{li}\right)}{N_s\,(1-\tau) \left(\sum\limits_{i=1}^{N_s} \varpi_{li}\right)}. \tag{34}$$

Assuming the worst case which is that all the users in the EH zone are located on the zone boundary, i.e, $d_{li}^{-m} = r^{-m}$ and $\varpi_{li} = \varpi$, which provides a lower bound, the average harvested power can now be expressed as

$$\bar{P}_k = \frac{\varpi\eta\tau P_{nr} \left(\frac{\Gamma(2+N_r)}{\Gamma(N_r)} + N_r\,(N_s-1)\right)}{(1-\tau)\,N_s^2}. \tag{35}$$

From this relation, we notice that, the harvested power decreases with increasing the distance between the user and the closest RRH. Consequently, the radius of the EH zone, r, can be defined based on this relation and the required harvested power (P_{rq}) as

$$r = \sqrt[m]{\frac{\eta\tau P_{nr} \left(\frac{\Gamma(2+N_r)}{\Gamma(N_r)} + N_r\,(N_s-1)\right)}{P_{rq} N_s^2\,(1-\tau)}}. \tag{36}$$

Thus radius of the EH zones can be obtained based on the target spectral efficiency and the system parameters such as number of the RRHs antennas and the transmission power in the power transfer phase. For a given value of the transmission power P_{rn}, number of the RRH antennas N_r, users N_s, the path loss exponent m and the EH efficiency η, the EH zones radius r depends on the required harvested power which is dependent essentially on the target spectral efficiency. Higher spectral efficiency leads to increase in the required harvested power P_{rq} and reduce in the radius of EH zone, and Vice-versa. Therefore users located beyond r are not able to provide the target spectral efficiency, and they will be considered as interference zone users, where their performance depend on the received signals from other RRHs.

In general, from the expressions derived in this, and previous, sections we can observe the following notes. The spectral efficiency is dependent mainly on the value of the EH time τ. The optimal τ for a given users locations can by obtained by a simple one dimensional search over $0 < \tau < 1$. Therefore, the optimal value of τ can be obtained as

$$C^* = \max_{0<\tau<1} C \text{ in } ((11) \text{ and } (29)). \tag{37}$$

Hence, the optimal value of τ, for un-known and full known CSI cases, can be efficiently obtained by using the line search techniques such as golden section method. The overall steps to calculate the optimal value of τ is stated in Algorithm 1. It is known that, for the uni modal functions the golden section search converges to the global optimal point [44], [45]; Consequently, Algorithm 1 always converges to the optimal point [44], [45]. Number of iterations required in this method is $\log_2 \frac{1}{\epsilon}$, where ϵ is the tolerance [44], [45].

Actually, the optimal value of τ, for given values of the transmission power and number of the RRH antennas, depends essentially on the distance between the users and the RRHs. If the distance is short, optimal τ will be small because the required harvested energy can be attained in shorter time duration. However, if the users are located far away from the RRH, the optimal value of τ will be larger. Furthermore, it is clear that increasing the number of antennas N_r, power P leads to decrease the value of optima τ. It is worth noting that, due to the ZF precoding implemented at the RRH, the users can transmit their data using all the harvested power, and they will not cause any interference to each other.

Algorithm 1 Optimal Algorithm for τ^*

Initialize $\varrho = 0$, $\beta = 1$, and $\Xi = \frac{-1+\sqrt{5}}{2}$.
Repeat
Update $\tau_1 = \varrho + (1-\Xi)\beta$ and $\tau_2 = \beta + (1-\Xi)\varrho$.
Obtain $C(\tau_1)$ and $C(\tau_2)$ from (11) and (29).
If $C(\tau_1) > C(\tau_2)$, set $\varrho = \tau_1$. Else set $\beta = \tau_2$.
Until $|\varrho - \beta|$ converges.
Find $\tau^* = (\varrho + \beta)/2$.

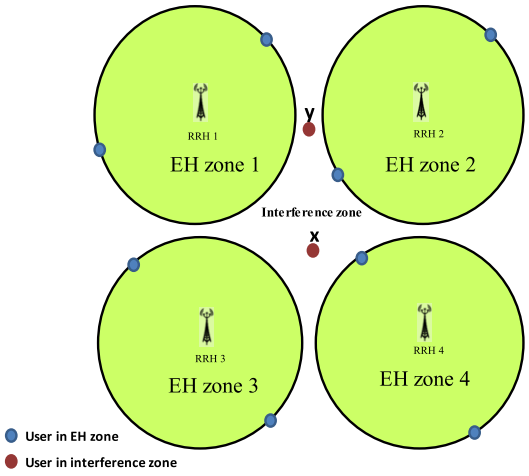

Fig. 3. EH-DAS with EH and interference zones.

V. Numerical Results

In this section, the derived analytical expressions are verified via Monte-Carlo simulation. Unless it is mentioned otherwise,

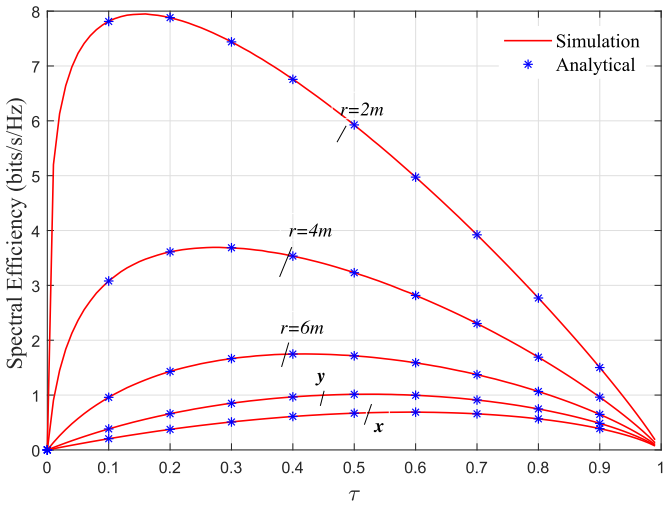

(a) Spectral Efficiency versus τ for Un-known CSI.

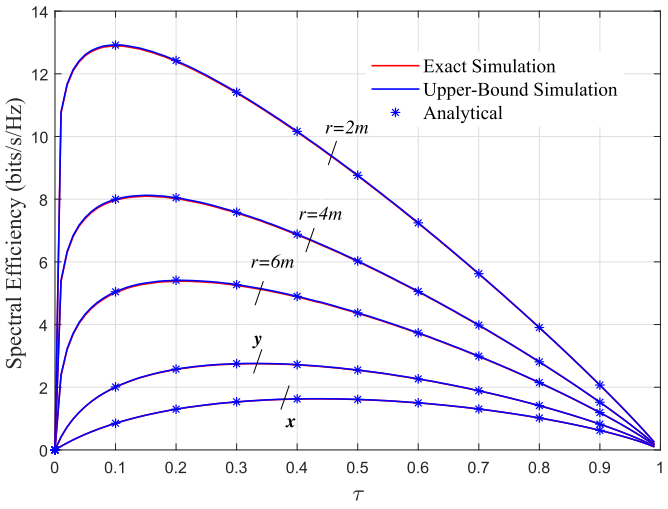

(b) Spectral Efficiency versus τ for Full-Known CSI.

Fig. 4. Spectral Efficiency versus τ for Different Users Locations.

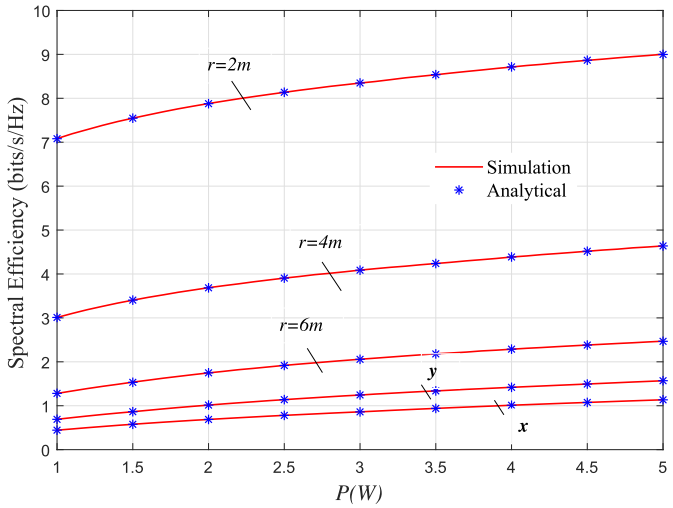

(a) Spectral Efficiency versus P for Un-known CSI, when $N_r = 100$.

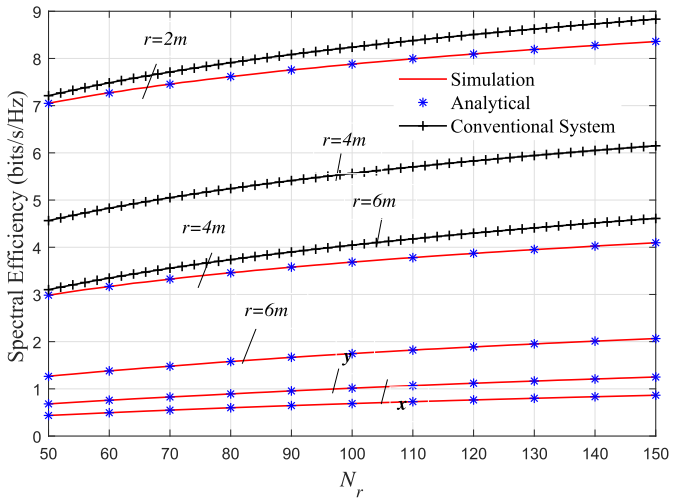

(b) Spectral Efficiency versus N_r for Un-known CSI, when $P = 2W$ and the users power in conventional system is $0.02W$.

Fig. 5. Spectral Efficiency versus P and N_r for Different Users Locations in Un-known CSI.

the path-loss exponent is $m = 2.7$, EH-receiver efficiency $\eta = 0.8$ [9], [31], and the noise power at all nodes is set as $\sigma^2 = -30$ dBw. In this section, we study DAS network illustrated in Fig. 3, where the RRHs 1, 2, 3 and 4 are connected to the CPU, i.e., $L = 4$, the inter-site distance between any two cooperative RRHs is 20 meters, the four cooperative RRHs form a square, number of the users $N_s = 10$, 2 users are located at the boundary of each EH zone of the RRHs and 2 users are located at positions $\mathbf{x}$ and $\mathbf{y}$ in the interference zone, where $\mathbf{x}$ is at the center of the square and $\mathbf{y}$ is at the mid-distance between two RRHs as in the figure. In addition, it is assumed that each user in the EH zone harvests energy and transmit its data from/to the closest RRH only, i.e, using only one RRH in the derived expressions for users in EH zones, while the users in interference zone harvest energy and transmit data to the all RRHs in the system.

Firstly, in order to explain the effect of the EH time duration, the ergodic spectral efficiency is plotted in Fig. 4 with respect to τ, when the radius of EH-zone $r = 2\,m, 4\,m$ and $6\,m$ for a user in EH-zone, and when EH-zone radius $r = 6\,m$ for the users in interference zone, when $P = 2W$ and $N_r = 100$. The results reveal that, the ergodic spectral efficiency degrades with increasing the distance. This is because increasing the path-loos implies decreasing the amount of the harvested power at each user. The other observation is that, there is an optimal value of the EH time τ^*, for each user location, that maximizes the system performance. However, interestingly enough, this optimal value τ^* becomes smaller when the user is closer to the RRHs. This can be intuitively explained as follows; reducing the distance means more harvested power at the users and hence the users require smaller amount of τ to reach their optimal performance. Final observation from these

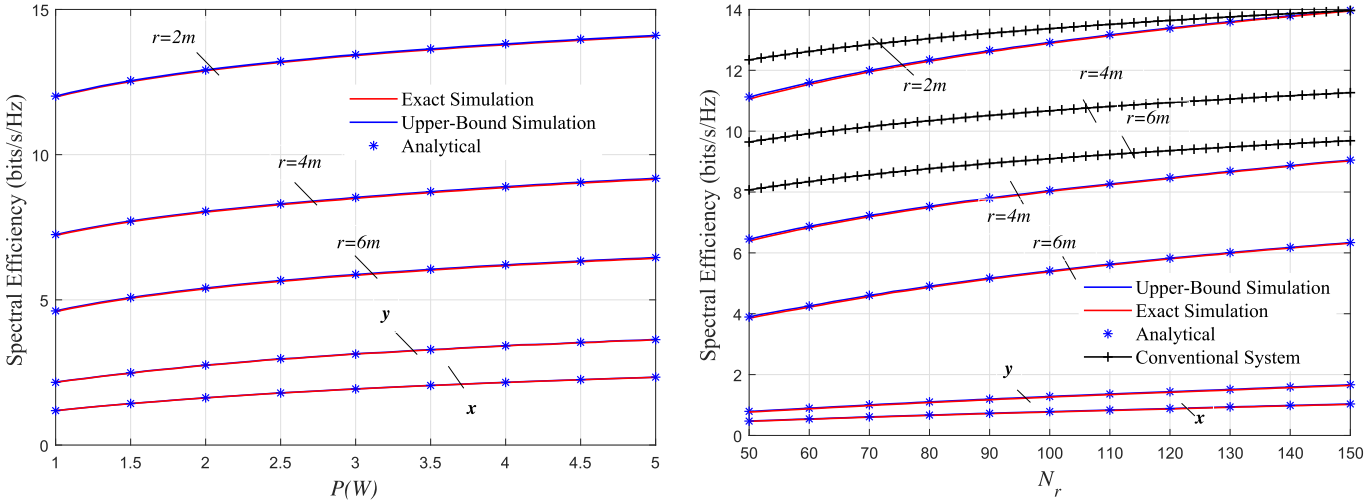

(a) Spectral Efficiency versus P for Full-known CSI, when$N_r = 100$.

(b) Spectral Efficiency versus N_r for Full-known CSI, when $P = 2W$ and the users power in conventional system is $0.7W$.

Fig. 6. Spectral Efficiency versus P and N_r for Different Users Locations in Full-known CSI.

results, the optimal EH-time τ^* is smaller in case when full-CSI is available. This is because MRT scheme can concentrate the transmitted power in the users directions, and as a result, smaller $\tau^*$is needed to reach the optimal spectral efficiency. Final remark as we can see from Fig. 4b the upper-bound and the actual spectral efficiency is tight under the system parameters considered in this section.

In order to explain the effect of the RRH power and number of RRH antennas on the proposed model. We illustrate in Fig. 5 and Fig. 6 the ergodic spectral efficiency as a function of P and N_r, respectively, for the two cases: unknown CSI and full known CSI. For comparison's sake, results for the conventional system where the users in the EH-zone area are not EH nodes, i.e., the users have fixed power supply, as studied in [18] are also included in Fig. 5b and Fig. 6b. It is clearly visible from the two figures that the spectral efficiency, in general, degrades with decreasing the RRH power and number of RRH antennas. This is because increasing P and/or N_r results in increasing the amount of the harvested energy at the energy constrain users. The other observation is that, the value of the EH-zone radius r is dependent on the required spectral efficiency of the users in this area which is dependent on the threshold requirements of the EH circuits at the users in this area. It can be clearly seen that, the maximum performance of the users in EH-zone degrades as the EH-zone area increases due to the path loss. However, amount of this degradation decreases as the EH-zone radius increases, as we can notice from the figures that, the gap between $r = 2m$ to $4m$ is wider than that when the radius changes from $r = 4m$ to $6m$.

In addition, comparing the spectral efficiency of the users in interference zone, it is clear that the users in the center of the interference zone have always lower spectral efficiency and the users in the areas between any two RRHs have highest spectral efficiency. Therefore, it is more efficient to add another RRH at the mid of the square (at the center). It is worthy to state that, the spectral efficiency of the users located in the interference zone plotted in Fig.6a when $r = 6m$ and in Fig. 6b when $r = 2m$; It is obvious from the figures that the spectral efficiency of the users in interference zone when $r = 6m$ is higher than that when $r = 2m$, which is expected because maximizing the harvested energy at the users in EH-zone who located at $r = 6m$ will lead also to increase the harvested power at the other users in the interference zone. As consequence, in full-known CSI, increasing the radius of EH-zone degrades the spectral efficiency of the users in EH-zone and enhances the spectral efficiency of the other users in interference zone.

Comparing the system model under consideration with the conventional system, one can notice that, the gap performance between the EH-DAS system and conventional DAS system becomes wider as the radius of the EH zone area increases, for instance the gap between the EH-DAS and conventional DAS when $r = 4m$ is wider than that when $r = 2m$. However, interestingly enough, increasing number of the RRH antennas N_r has different impact on the gap performance between the two systems. On one hand, in the un-known CSI increasing N_r leads to increase the gap performance between the two systems, this can be seen clearly in case when $r = 2m$ in Fig. 5b. On the second hand, in full known CSI increasing N_r results in reducing the gap performance between the two systems, this also is clear in case when $r = 2m$ in Fig. 6b.

Final remark and as anticipated that, the system performance in the second case when the CSI is fully known much better than that when the CSI is un-known in the charging time slot.

In Fig. 7, we plot the maximum average harvested power of the users in EH zones versus the RRHs power in the first phase, when $N_r = 100$ and $\eta = 1$ for different values of the EH zone radius $r = 2m$ and $4m$. Generally and as we can see from the figure that, the average harvested power in full-known CSI scheme is higher than that in the un-known CSI scheme. In addition, decreasing the EH zone area increases amount

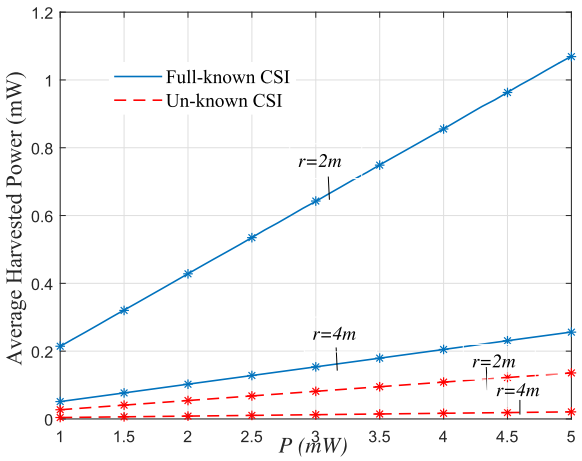

Fig. 7. Harvested Power versus P in the two schemes.

of the harvested power at the users, and this enhancement in the amount of the harvested power is essential when the RRHs power is high.

VI. Conclusions

In this work, we have proposed using the distributed RRHs in DAS systems to transmit signals and also to power the energy-constrained users, where each RRH has an EH-zone. Harvest-then transmit protocol was assumed and the spectral efficiency was considered when the ZF receiver is implemented at the RRHs in two scenarios, namely, 1) unknown CSI 2) full-known CSI in the charging time slot. New exact and bound expressions for the ergodic spectral efficiency of the proposed EH-DAS system have been obtained for each scenario, which then confirmed by Monte-Carlo simulations. Then, the impact of different system-parameters, such as time duration of EH phase, and the value of the RRHs power and antennas, on the performance of the considered DAS-MIMO system have been investigated. It was shown that, increasing P and/or N_r always enhance the system performance and the duration of the EH-time slot is main factor to obtain the optimal performance. In addition, in full-known CSI increasing the EH-zone radius degrades the spectral efficiency of the users in EH-zone and enhances the spectral efficiency of the users in interference-zone.

References

[1] L. R. Varshney, "Transporting information and energy simultaneously," in *Proc. IEEE Int. Symp. Inf. Theory (ISIT)*, Jul. 2008, pp. 1612–1616.
[2] P. Grover and A. Sahai, "Shannon meets Tesla: Wireless information and power transfer," in *Proc. IEEE Int. Symp. Inf. Theory (ISIT)*, Jun. 2010, pp. 2363–2367.
[3] X. Zhou, R. Zhang, and C. K. Ho, "Wireless information and power transfer: Architecture design and rate-energy tradeoff," *IEEE Trans. Commun.*, vol. 61, no. 11, pp. 4754–4767, Nov. 2013.
[4] L. Liu, R. Zhang, and K.-C. Chua, "Wireless information transfer with opportunistic energy harvesting," *IEEE Trans. Wireless Commun.*, vol. 12, no. 1, pp. 288–300, Jan. 2013.
[5] W. Huang, H. Chen, Y. Li, and B. Vucetic, "On the performance of multi-antenna wireless-powered communications with energy beamforming," *IEEE Trans. Veh. Technol.*, vol. 65, no. 3, pp. 1801–1808, Mar. 2016.
[6] G. L. Moritz, J. L. Rebelatto, R. D. Souza, B. Uchôa-Filho, and Y. Li, "Time-switching uplink network-coded cooperative communication with downlink energy transfer," *IEEE Trans. Signal Process.*, vol. 62, no. 19, pp. 5009–5019, Oct. 2014.
[7] H. Ju and R. Zhang, "Throughput maximization in wireless powered communication networks," *IEEE Trans. Wireless Commun.*, vol. 13, no. 1, pp. 418–428, Jan. 2014.
[8] L. Liu, R. Zhang, and K.-C. Chua, "Multi-antenna wireless powered communication with energy beamforming," *IEEE Trans. Commun.*, vol. 62, no. 12, pp. 4349–4361, Dec. 2014.
[9] A. Salem and K. A. Hamdi, "Wireless power transfer in multi-pair two-way AF relaying networks," *IEEE Trans. Commun.*, vol. 64, no. 11, pp. 4578–4591, Nov. 2016.
[10] S. Timotheou, I. Krikidis, G. Zheng, and B. Ottersten, "Beamforming for MISO interference channels with QoS and RF energy transfer," *IEEE Trans. Wireless Commun.*, vol. 13, no. 5, pp. 2646–2658, May 2014.
[11] M.-M. Zhao, Q. Shi, Y. Cai, and M.-J. Zhao, "Joint transceiver design for full-duplex cloud radio access networks with swipt," *IEEE Trans. Wireless Commun.*, vol. 16, no. 9, pp. 5644–5658, Sep. 2017.
[12] K. Huang, C. Zhong, and G. Zhu, "Some new research trends in wirelessly powered communications," *IEEE Wireless Commun.*, vol. 23, no. 2, pp. 19–27, Apr. 2016.
[13] D. W. K. Ng and R. Schober, "Secure and green SWIPT in distributed antenna networks with limited backhaul capacity," *IEEE Trans. Wireless Commun.*, vol. 14, no. 9, pp. 5082–5097, Sep. 2015.
[14] D. Lee *et al.*, "Coordinated multipoint transmission and reception in LTE-advanced: Deployment scenarios and operational challenges," *IEEE Commun. Mag.*, vol. 50, no. 2, pp. 148–155, Feb. 2012.
[15] R. Irmer *et al.*, "Coordinated multipoint: Concepts, performance, and field trial results," *IEEE Commun. Mag.*, vol. 49, no. 2, pp. 102–111, Feb. 2011.
[16] D. W. K. Ng, E. S. Lo, and R. Schober, "Energy-efficient resource allocation in multi-cell OFDMA systems with limited backhaul capacity," *IEEE Trans. Wireless Commun.*, vol. 11, no. 10, pp. 3618–3631, Oct. 2012.
[17] D. Wang, J. Wang, X. You, Y. Wang, M. Chen, and X. Hou, "Spectral efficiency of distributed MIMO systems," *IEEE J. Sel. Areas Commun.*, vol. 31, no. 10, pp. 2112–2127, Oct. 2013.
[18] H. B. Almelah and K. A. Hamdi, "Spectral efficiency of distributed large-scale MIMO systems with ZF receivers," *IEEE Trans. Veh. Technol.*, vol. 66, no. 6, pp. 4834–4844, Jun. 2017.
[19] E. Park, S. R. Lee, and I. Lee, "Antenna placement optimization for distributed antenna systems," *IEEE Trans. Wireless Commun.*, vol. 11, no. 7, pp. 2468–2477, Jul. 2012.
[20] L. Dai, "An uplink capacity analysis of the distributed antenna system (DAS): From cellular DAS to DAS with virtual cells," *IEEE Trans. Wireless Commun.*, vol. 13, no. 5, pp. 2717–2731, May 2014.
[21] H. Ren, N. Liu, C. Pan, and C. He, "Energy efficiency optimization for MIMO distributed antenna systems," *IEEE Trans. Veh. Technol.*, vol. 66, no. 3, pp. 2276–2288, Mar. 2017.
[22] H. Kim, E. Park, H. Park, and I. Lee, "Beamforming and power allocation designs for energy efficiency maximization in MISO distributed antenna systems," *IEEE Commun. Lett.*, vol. 17, no. 11, pp. 2100–2103, Nov. 2013.
[23] S.-R. Lee, S.-H. Moon, H.-B. Kong, and I. Lee, "Optimal beamforming schemes and its capacity behavior for downlink distributed antenna systems," *IEEE Trans. Wireless Commun.*, vol. 12, no. 6, pp. 2578–2587, Jun. 2013.
[24] H. Tabassum and E. Hossain, "On the deployment of energy sources in wireless-powered cellular networks," *IEEE Trans. Commun.*, vol. 63, no. 9, pp. 3391–3404, Sep. 2015.
[25] G. Zhao and C. Zhang, "Improving wireless power transfer via power beacons with circularly distributed antennas," in *Proc. 8th Int. Conf. Wireless Commun. Signal Process. (WCSP)*, Oct. 2016, pp. 1–5.
[26] Y. Huang, M. Liu, and Y. Liu, "Energy-efficient SWIPT in IoT distributed antenna systems," *IEEE Internet Things J.*, vol. 5, no. 4, pp. 2646–2656, Aug. 2018.
[27] F. Yuan, S. Jin, K.-K. Wong, J. Zhao, and H. Zhu, "Wireless information and power transfer design for energy cooperation distributed antenna systems," *IEEE Access*, vol. 5, pp. 8094–8105, 2017.
[28] S. Lee and R. Zhang, "Distributed wireless power transfer with energy feedback," *IEEE Trans. Signal Process.*, vol. 65, no. 7, pp. 1685–1699, Apr. 2017.
[29] F. Yuan, S. Jin, Y. Huang, K.-K. Wong, Q. T. Zhang, and H. Zhu, "Joint wireless information and energy transfer in massive distributed antenna systems," *IEEE Commun. Mag.*, vol. 53, no. 6, pp. 109–116, Jun. 2015.
[30] G. Wang, C. Meng, W. Heng, and X. Chen, "Secrecy energy efficiency optimization in an-aided distributed antenna systems with energy harvesting," *IEEE Access*, vol. 6, pp. 32830–32838, 2018.

[31] X. Chen, C. Yuen, and Z. Zhang, "Wireless energy and information transfer tradeoff for limited-feedback multiantenna systems with energy beamforming," *IEEE Trans. Veh. Technol.*, vol. 63, no. 1, pp. 407–412, Jan. 2014.
[32] Y. Zeng and R. Zhang, "Optimized training design for wireless energy transfer," *IEEE Trans. Commun.*, vol. 63, no. 2, pp. 536–550, Feb. 2015.
[33] C.-F. Liu, M. Maso, S. Lakshminarayana, C.-H. Lee, and T. Q. S. Quek, "Simultaneous wireless information and power transfer under different CSI acquisition schemes," *IEEE Trans. Wireless Commun.*, vol. 14, no. 4, pp. 1911–1926, Apr. 2015.
[34] J. Xu and R. Zhang, "Energy beamforming with one-bit feedback," *IEEE Trans. Signal Process.*, vol. 62, no. 20, pp. 5370–5381, Oct. 2014.
[35] G. Yang, C. K. Ho, and Y. L. Guan, "Dynamic resource allocation for multiple-antenna wireless power transfer," *IEEE Trans. Signal Process.*, vol. 62, no. 14, pp. 3565–3577, Jul. 2014.
[36] K. A. Hamdi, "A useful lemma for capacity analysis of fading interference channels," *IEEE Trans. Commun.*, vol. 58, no. 2, pp. 411–416, Feb. 2010.
[37] G. Amarasuriya, C. Tellambura, and M. Ardakani, "Sum rate analysis of two-way MIMO AF relay networks with zero-forcing," *IEEE Trans. Wireless Commun.*, vol. 12, no. 9, pp. 4456–4469, Sep. 2013.
[38] M. Abramowitz and I. A. Stegun, *Handbook of Mathematical Functions With Formulas, Graphs, and Mathematical Tables*. Washington, DC, USA: Department of Commerce, 1972.
[39] H. Tabassum, E. Hossain, A. Ogundipe, and D. I. Kim, "Wireless-powered cellular networks: Key challenges and solution techniques," *IEEE Commun. Mag.*, vol. 53, no. 6, pp. 63–71, Jun. 2015.
[40] A. M. Tulino and S. Verdú, *Random Matrix Theory and Wireless Communications*. Amsterdam, The Netherlands: Now, 2004.
[41] G. Zhu, C. Zhong, H. A. Suraweera, Z. Zhang, and C. Yuen, "Outage probability of dual-hop multiple antenna AF systems with linear processing in the presence of co-channel interference," *IEEE Trans. Wireless Commun.*, vol. 13, no. 4, pp. 2308–2321, Apr. 2014.
[42] H. Q. Ngo, E. G. Larsson, and T. L. Marzetta, "Energy and spectral efficiency of very large multiuser MIMO systems," *IEEE Trans. Commun.*, vol. 61, no. 4, pp. 1436–1449, Apr. 2013.
[43] J. Cui and A. U. H. Sheikh, "Outage probability of cellular radio systems using maximal ratio combining in the presence of multiple interferers," *IEEE Trans. Commun.*, vol. 47, no. 8, pp. 1121–1124, Aug. 1999.
[44] J. Kim, H. Lee, C. Song, T. Oh, and I. Lee, "Sum throughput maximization for multi-user MIMO cognitive wireless powered communication networks," *IEEE Trans. Wireless Commun.*, vol. 16, no. 2, pp. 913–923, Feb. 2017.
[45] H. Lee, K. J. Lee, H. B. Kong, and I. Lee, "Sum-rate maximization for multiuser MIMO wireless powered communication networks," *IEEE Trans. Veh. Technol.*, vol. 65, no. 11, pp. 9420–9424, Nov. 2016.

Abdelhamid Salem (S'12) received the B.Sc. degree in electrical and electronic engineering from the University of Benghazi, Benghazi, Libya, in 2002, the M.Sc. degree (Hons.) in communication engineering from the University of Benghazi in 2009, and the Ph.D. degree in electrical and electronic engineering from Manchester University, Manchester, in 2017. He is currently a Research Fellow with the Department of Electronic and Electrical Engineering, University College London, U.K. He was a Post-Doctoral Researcher with the School of Computer Science and Electronic Engineering, University of Essex, U.K., and a Research Assistant with the School of Electrical and Electronic Engineering, The University of Manchester, U.K.

His current research interests include energy harvesting, wireless power transfer, MIMO systems, physical layer security, and signal processing for interference mitigation and power line communications.

Leila Musavian (S'05–M'07) received the Ph.D. degree in telecommunications from King's College London, U.K. She is currently a Reader with the School of Computer Science and Electrical Engineering, University of Essex. Prior to that, she was a Lecturer with InfoLab21, Lancaster University (2012–2016). She was a Research Associate with McGill University (2011–2012), Canada, where she was also a Post-Doctoral Fellow with INRS-EMT from 2006 to 2008. Her research interests lie in 5G/B5G, radio resource management for next generation wireless networks, CRNs, energy harvesting, green communication, energy-efficient transmission techniques, and cross-layer design for delay QoS provisioning and 5G systems. She is currently an Editor of the IEEE TRANSACTIONS ON WIRELESS COMMUNICATIONS, the Executive Editor of the *Transactions on Emerging Telecommunications Technologies*, and an Associate Editor of the *Internet Technology Letters* (Wiley).

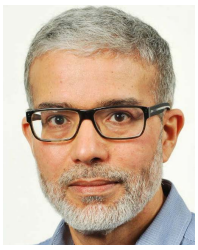

Khairi Ashour Hamdi (M'99–SM'02) received the B.Sc. degree in electrical engineering from Alfateh University, Tripoli, Libya, in 1981, the M.Sc. degree (Hons.) from the Technical University of Budapest, Budapest, Hungary, in 1988, and the Ph.D. degree in telecommunication engineering from the Hungarian Academy of Sciences in 1993. His current research interests include modeling and performance analysis of wireless communication systems and networks, green communication systems, and heterogeneous mobile networks.